Bulletin of Electrical Engineering and Informatics
Vol. 9, No. 6, December 2020, pp. 2601~2608
ISSN: 2302-9285, DOI: 10.11591/eei.v9i6.2624

Photoacoustic technology for biological tissues characterization

Hui Ling Chua, Audrey Huong
Department of Electronic Engineering, Universiti Tun Hussein Onn Malaysia, Malaysia

Article Info

Article history:

Received Mar 30, 2020
Revised May 2, 2020
Accepted May 30, 2020

Keywords:

Biological tissue
Optical absorption
Phase
Photoacoustic imaging
SNR

ABSTRACT

The existing photoacoustics (PA) imaging systems showed mixed performance in imaging characteristic and signal-to-noise ratio (SNR). This work presents the use of an in-house assembled PA system using a modulating laser beam of wavelength 633 nm for two-dimensional (2D) characterization of biological tissues. The differentiation of the tissues in this work is based on differences in their light absorption, wherein the produced photoacoustic signal detected by a transducer was translated into phase value that corresponds to the peak amplitude of optical absorption of tissue namely fat, liver and muscle. This work found fat tissue to produce the strongest PA signal with mean ± standard deviation (SD) phase value = 2.09 ± 0.31 while muscle produced the least signal with phase value = 1.03 ± 0.17. This work discovered the presence of stripes pattern in the reconstructed images of fat and muscle resulted from their structural properties. In addition, a comparison is made in an attempt to better assess the performance of the developed system with the related ones. This work concluded that the developed system may use as an alternative, noninvasive and label-free visualization method for characterization of biological tissues in the future.

This is an open access article under the CC BY-SA license.

Corresponding Author:

Audrey Huong,
Department of Electronic Engineering,
Universiti Tun Hussein Onn Malaysia,
86400 Parit Raja, Johor, Malaysia.
Email: audrey@uthm.edu.my

1. INTRODUCTION

Imaging is a process of producing a visual representation of a scanned object through the combined technology of electromagnetic beam illumination and signal detection. The action or process of producing an image of a part of human body using radiographic techniques has greatly advanced in clinical settings, which primarily focus is on diagnostic and therapeutic use to verify the origins of an injury. Over the years, a variety of imaging techniques are available for the same purpose such as magnetic resonance imaging (MRI), X-ray computed tomography (CT), ultrasound and spectroscopy. These imaging techniques are used to generate visual representation of body parts and to aid in clinical diagnosis. However, the operation of most of these machines can be time consuming and expensive. In addition exogenous dye is often required in MRI and CT to enhance contrast in imaging.

PA technology was discovered in year 1880 by A. G. Bell through his photophone invention [1]. This is a hybrid method that combines optical and acoustic approach. Unlike ultrasound technique, which exhibits a tradeoff between imaging resolution and penetration depth [2], PA offers greater specificity with the ability to detect hemoglobin, lipids, water and other light-absorbing chromophores, compounded with greater resolution than its ultrasonic counterpart. The PA strategy is attainable by the use of light source of non-ionizing laser pulses for illumination of biological tissues. The absorbed light energy produced thermal expansion within the medium, and hence generation of acoustic waves. This thermal waves propagation

is affected by the (arrival) elevation angle and velocity of the wave signal; both of which parameters influence phase shift of the wave detected using a transducer [3]. These attributes lead to the use of PA imaging in a wide variety of applications in clinical study [4], preclinical research and basic biology for studying cancer [5], cardiovascular disease [6], abnormalities of the microcirculation [7] and other conditions. However the current market available PA systems are bulky, costly (costing about USD 230,000), and some of them may require the use of contrast agents for enhanced visualization**,** which preparation process can be complicated [8]. To date, there are mixed reports on the performance of these system. Erfanzadeh *et al.* [9] reported a relatively low SNR of approximately 14 dB for *ex vivo* imaging of mouse ear, while Upputuri *et al*. [10] stated the need of using indocyanine green (ICG) for 3 cm depth imaging of chicken breast tissue. A similar work by Manojit *et al*. [11] showed a near real time imaging (~3 s) of small field of views (FOVs) to produce images of SNR 15 dB. It is, therefore, the aim of this work to investigate the feasibility of using a low cost laboratory-assembled PA system for marker-free 2D optical characterization of biological tissues, and to better understand where our system stands in the current field.

2. RESEARCH METHOD

2.1. Photoacoustic system and poultry sample preparation

The employed PA imaging system consists of three main parts: temporally modulated laser source, ultrasonic transducer and two-dimensional (2D) positional stage. A continuous wave laser source (model no. R-30993, Newport Corporation) of center wavelength, λ, 633 nm was allowed to pass through an acousto-optic modulator (AOM) (model: Gooch & Housego 2910 series) producing trains of laser pulses for illumination of the chosen sample. The AOM controlled by a radiofrequency (RF) driver shown in Figure 1 was driven by a frequency of 15 MHz generated using a function generator (model no. YOKOGAWA FG 39).

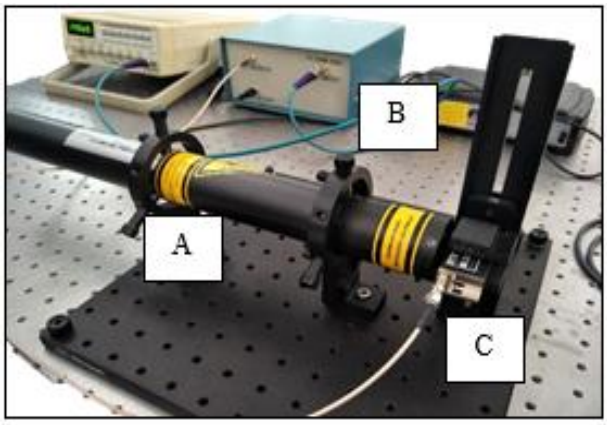

Figure 1. Light modulating system, (a) Laser source, (b) RF driver,
(c) Acousto-optic modulator (AOM)

Meanwhile the detection of PA signals produced by the investigated sample was by an unfocused ultrasonic linear array transducer (model no. LF 2000K1, central frequency, f_c = 2 MHz) connected to an oscilloscope (model no. HMO2022, Rohde & Schwarz) for acquisition and offline transfer of data. This system was developed at a fractional cost of the existing systems (costing approximately USD 9,200). It was reported in [12] that both the optical and acoustic characteristics of muscle samples resemble to that of human breast and breast tumors. In addition the International Chicken Genome Sequencing Consortium revealed chickens to share 60 % of the same genes as that of humans [13], therefore samples of muscle, fatty tissue and liver were extracted from chicken carcasses and used in the present investigation. The thickness of these prepared samples was approximately 3 mm while the width was 2 cm similar to the transducer diameter shown in Figure 2. This selection of the sample width is following the findings by [14] as an important parameter for optimal longitudinal attenuation measurement. The investigated samples were submerged in water, which is used as the medium of propagation between transducer and the sample, and the separation between the transducer and investigated tissue sample was approximately 2 cm. In this study, twenty sets of experiments were conducted on each considered tissue sample at different location to give a total of 60 sets of data. The acquisition time for each point was approximately 2 seconds.

2.1. Data collection and analytical technique

The signal phase shift is based on thermal wave propagation, where its amplitude has strong dependence on surface temperature, which can be affected by environmental reflections, non-uniform heating and emissivity variations [15]. The PA signals collected from each experiment were recorded and extracted for the Φ value from the peak of the manipulated signals. Each reconstructed image was given from a series of 20 sampled signals collected at a rotating resolution of 18^o/step (i.e. spatial resolution of 2 mm), and at 10 s delay between each measurement. The transducer attached to the shaft of the rotational motor (model no. ELLO 8 Thorlabs) to provide 2D measurement of data and an illustration of the system deployed for this research study is shown in Figure 2.

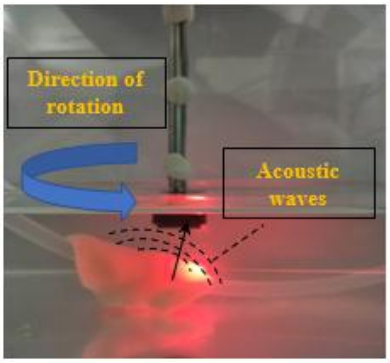

Figure 2. The collection of spatial-resolved PA signals via rotation motion of transducer

The peak phase value was extracted for all angles for construction of 2D image data. The processing of the measured acoustic signals is by Fast-Fourier transform (FFT) technique, which allows transformation of time domain signals to that of frequency domain. This study used *fft* function available in MATLAB software (version 2016a) given in (1) to give both real (*re*) and imaginary parts (*im*) of the acoustic signals, using which the Φ value is calculated. The latter is corresponded to the absorption properties of the investigated medium, wherein the higher the value the greater the light absorption.

$$(\Psi_{re,} \Psi_{im}) = fft\,(\psi(t)) \quad (1)$$

where $\psi(t)$ represents acoustic wave in time domain, while Ψ_{re} and Ψ_{im} represent the frequency domain signal in the form of complex number. The Φ value, in unit of rad, is given by the peak of *re* and *im* components of the transformed data as follows:

$$\Phi = \tan\left(\frac{\psi_{im}}{\psi_{re}}\right) \quad (2)$$

Using the data collected, the maximum Φ value of each signal was calculated and arranged in matrix format before spline interpolation (*interp2*, interpolation factor of 10) was performed for interpolating and smoothing the image data. The results of the proposed technique were evaluated using image quality metric, specifically the SNR. The SNR is calculated as the logarithmic ratio of mean signal, $I_{M,}$ to its SD, $I_{SD,}$ given in (3) in units of decibel (dB). It was reported in Konrad *et al*. [16] that excellent image quality yields SNR value of 32 dB, while 26 dB can be expected to be of acceptable quality.

$$\text{SNR} = 10 \log (I_M / I_{SD}) \quad (3)$$

3. RESULTS AND DISCUSSION

Example of PA signals at arbitrarily selected sequential angle of 0^o, 90^o, 180^o and 270^o recorded for liver tissue according to the method described in section 2.2 is shown in Figure 3. These data were then arranged in two-dimensional arrays producing 2D Φ images of liver calculated from (2). The same procedure was repeated for fat and muscle samples. An example of the processed image from signals collected from fat, liver and muscle are shown in Figures 4, 5 and 6, respectively. These Φ images comprised of spatial

distribution of pixels of different intensity, which corresponded linearly to the detected acoustic strength. It must be mentioned that the results presented in this work is valid for the transducer model employed herein as it was reported that the shape of transducer (most often available in either rectangular or round shape), even of the same operating frequency and diameter, would exhibit a different beam detection profile [12, 17, 18].

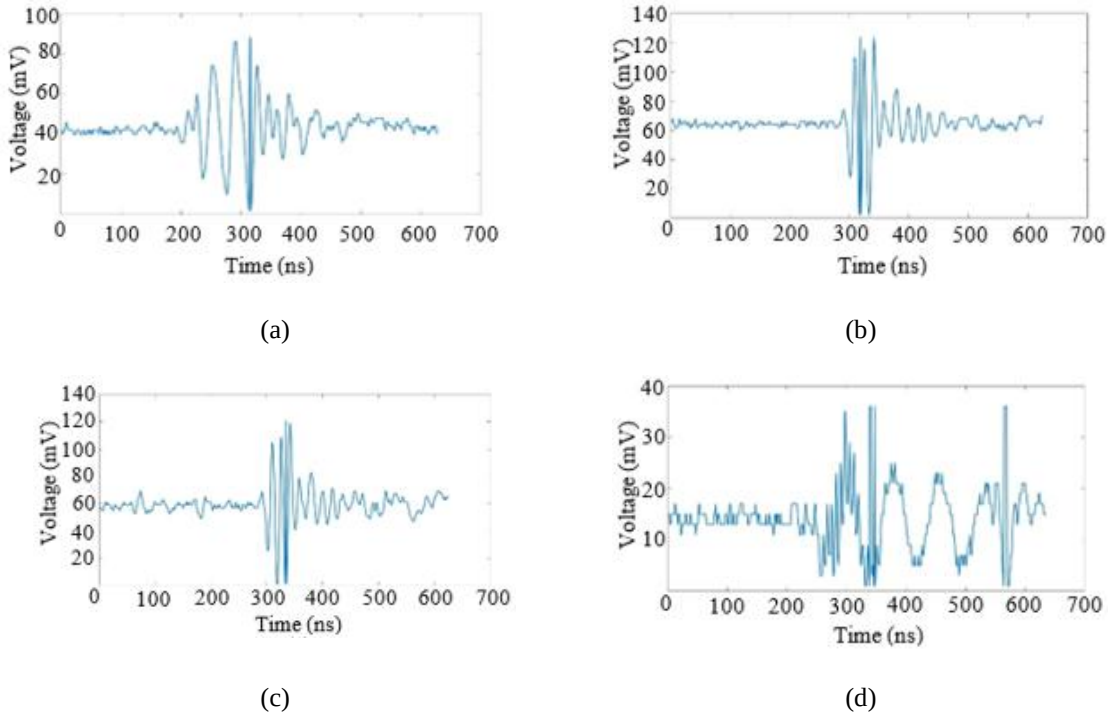

Figure 3. PA signals recorded for liver tissue at rotating angle of, (a) 0^o, (b) 90^o, (c) 180^o, (d) 270^o

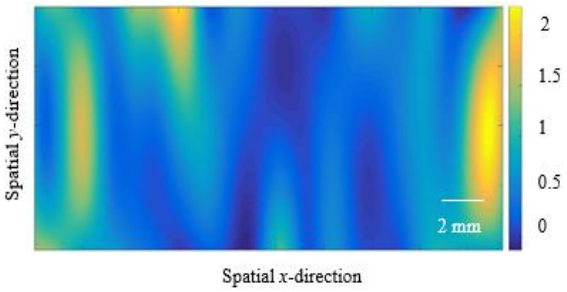

Figure 4. Smoothed reconstructed image for signals collected from fat sample

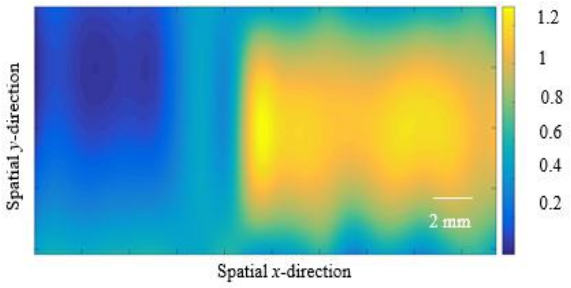

Figure 5. Smoothed reconstructed image for signals collected from liver

It is interesting to note that even though without the use of a contrast dye, lines and stripes pattern can be visibly seen in fat and muscle samples shown in Figure 4 and Figure 6. Chicken fats are of lipids with the presence of cuticle on its surface, and comprises of a thin outer layer overlaying the thick inner layer [19] while the patterns observed for muscle sample are likely due to the presence of fibre and collagen tissues available in abundance on the poultry surface. Since liver exhibits smooth surface, these patterns were not observed in the corresponding sample. Meanwhile possible explanations on the variation in the distribution of PA signals are provided in the following using result from liver as an example. The intensity of value ranges in between 0-0.30 rad in Figure 7 is likely caused by the reflections of light from the water tank glass, which values vary gradually over the range of angles subtended by the transducer [20, 21]. This was verified using an experiment on a diffuser glass submerged in water to create scattering effect within the medium before measurement of PA signal and phase value was calculated (results not shown here).

It was found that the mean and SD of Φ value under this condition was calculated as 0.20 ± 0.08 rad, which range is similar to that hypothesized as light reflections in this work. Meanwhile high intensity region in Figure 7 is corresponded to the region that has the greatest light beam exposure, which leads to the highest light absorption. This produced the highest calculated Φ signals ranged between 0.80-1.20 rad. There are also regions, which phase values range between 0.40-0.80 rad, corresponded to acoustic signals produced through weaker light intensity exposure coupled with the scattering effects.

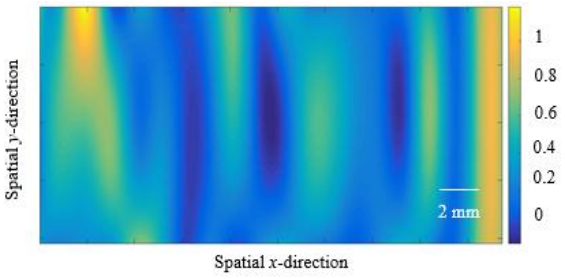

Figure 6. Smoothed reconstructed image for signals collected from muscle sample

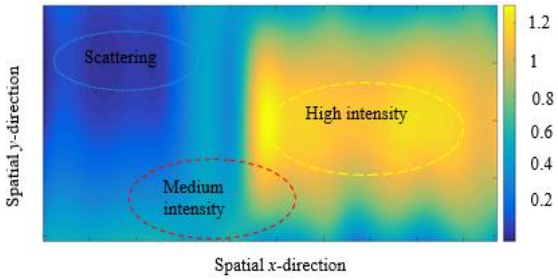

Figure 7. Effects of light absorption and scattering on the calculated phase value

From the results in Figures 4-6, fatty tissues were found to produce the largest average PA signals with mean ± SD of Φ = 2.09 ± 0.31, whereas muscle produced the least signals with Φ = 1.03 ± 0.17. These differences in phase value range measured for fat and muscle sample can be contributed by the differences in the refractive index, *n*, of these samples given by 1.45 and 1.39, respectively. In addition to the differences in light scattering upon light incident at the samples surface, the velocity of propagating light waves reduces (at different rate depending on *n* value) in these media; this renders different light absorption by the tissues, thus variation in phase value calculated from the reflected signals. Previous work in [22] reported a complete separation of the image contrast can be reached based on the absorption and *n* value of the investigated sample. Regions with different *n* value would enhance the visibility of the edges in the constructed image; therefore fine details of sample structure could be observed without the use of stains and contrasts agents. Figure 8 showed the SNR value calculated for Φ images of liver, muscle and fatty tissues. Based on the results, the overall mean and SD of SNR is calculated as 29.37 dB ± 3.93 dB, which falls within the acceptable range. The results also showed that there are ten from 60 sets of Φ data that produced SNR below 26 dB, which can be contributed by artifact motion during data acquisition, hence giving a probability rate of good image quality (SNR ≥ 26 dB) of 83.33 %.

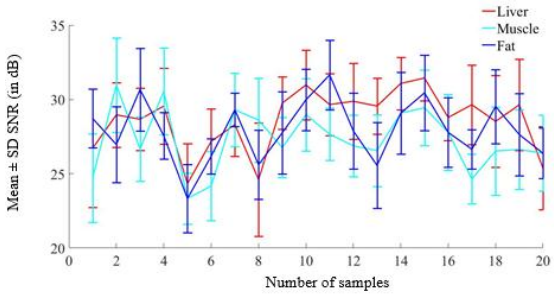

Figure 8. The mean and standard deviation (SD) of SNR of Φ data of liver (red line), muscle (turquoise line) and fat (blue line)

The results in Table 1 showed a compound influence of pixel size and scanning time on FOV size; this is in good agreement with that observed in [24-26] who also suggested an inverse relationship between the viewing size and spatial resolution. Other factors that could influence spatial resolution performance of a PA imaging system include magnification of focal spot [27] and the light beam pulse width [28]. A shorter pulse width is reported to produce an improved spatial resolution image [29], which is supported by the observations in the results from [26] in Table 1 as compared to that obtained in this work.

Table 1. A comparison of the performance of the developed system with other related works

Parameters	Previous works [ref]	This work
SNR	14-18 dB [9]	
	115-175 dB [10]	29.37 ± 3.93 dB
	~15-18 dB [11]	
	~17 dB [23]	
Spatial resolution	0.836 ×2.1 µm - 2.9 × 10.1 µm [9]	2000 µm
(pixel size)	285 - 435 µm [10]	
	180 - 384 µm [11]	
Scanning time	10 - 30 s [10]	40 s
(in seconds, s)	3 - 30 s [11]	
	5 s [23]	
Field of view	4.6 mm × 3.7 mm [9]	44 mm × 20 mm
	4.2 mm × 5 mm [10]	
	4.2 mm × 4.2 mm [11]	
	6 mm × 4.2 mm [23]	
Pulse width	50 ns [9]	30 ns
	136 ns [10]	
	136 ns [11]	
	5 ns [23]	

Since light scattering and absorbing (optical properties) in a turbid medium (e.g. biological tissue) leads to a reduce in the energy density [30], the amount of light reaching the detector (in reflectance mode) reduces significantly with an increase in imaging depth. The latter renders a decrease in SNR [31], unlike the works in [12] on PA imaging of horse hair phantom (of negligible thickness), most of the previous works in Table 1 showed a relatively consistent and lower SNR performance as compared to that obtained in this work (mean SNR of 29 dB) ranging between 14-18 dB for measurement on biological tissues. Nonetheless it must be mentioned that SNR performance would generally increase with FOV [32] at the price of a longer imaging time [33].

It has been noted in [34] that f_c and bandwidth of the employed ultrasound transducer is a significant factor affecting spatial resolution of an image. This could possibly explain the reason for the coarse pixel size identified in this works (using f_c of 2 MHz) as compared to the others such as [12] that used 2.25 MHz and 5 MHz. Unlike the study in [23] that used a focused transducer, the use of unfocused transducer in this work has the added advantage of a larger viewing angle, hence an increased viewing area (of up to 44 mm×20 mm). The results presented herein showed the feasibility of the developed system for noninvasive assessment of optical, physiological and structural properties of the investigated samples with reasonably acceptable performance, implying its potential application as a label-free technology using phase information of acoustic signal for biological tissues visualization [35].

4. CONCLUSION

The PA imaging technology presented in this work shows a great potential in medical imaging as this technology is able to produce images with acceptable imaging performance and SNR as compared to the existing systems. This work used a low cost PA imaging system for marker-free characterization and differentiation of biological samples based on the variations in their light absorption, which can be translated through the amplitude of the detected PA signals. This system is able to reveal the structural properties of the biological tissues with a relatively good overall mean and SD SNR of 29.37 ± 3.93 dB and cover a considerably large imaging area. The future works include the use of this photoacoustic system for physiological and pharmacological study by exploiting the photo-thermal properties of chromophores.

ACKNOWLEDGEMENTS

We are grateful to Universiti Tun Hussein Onn Malaysia under GPPS Grant Vot Number H 302 for financially supporting this work.

REFERENCES

[1] A. G. Bell, "ART. XXXIV.--On the Production and Reproduction of Sound by Light," *American Journal of Science (1880-1910)*, vol. 20, no. 118, pp. 305, 1880.

[2] C. Oates and P. Taylor, "Helping expectant mothers understand inadequate ultrasound images," *Ultrasound*, vol. 24, no. 3, pp. 142-146, 2016.

[3] Z. Liu, K. L. Koh, A. Mezentsev, S.-E. Enno, J. Sugier and M. Füllekrug, "Variable phase propagation velocity for long-range lightning location system," *Radio Science*, vol. 51, no. 11, pp. 1806-1815, 2016.
[4] J. L. Su, A. B. Karpiouk, B. Wang and S. Y. Emelianov, "Photoacoustic imaging of clinical metal needles in tissue," *Journal of biomedical optics*, vol. 15, pp. 021309, 2010.
[5] S. Mallidi, G. P. Luke and S. Emelianov, "Photoacoustic imaging in cancer detection, diagnosis, and treatment guidance," *Trends in biotechnology*, vol. 29, no. 5, pp. 213-221, 2011.
[6] B. Wang, J. L. Su, J. Amirian, S. H. Litovsky, R. Smalling and S. Emelianov, "Detection of lipid in atherosclerotic vessels using ultrasound-guided spectroscopic intravascular photoacoustic imaging," *Optics express*, vol. 18, no. 5, pp. 4889-4897, 2010.
[7] P. Beard, "Biomedical photoacoustic imaging," *Interface focus*, vol. 1, no. 4, pp. 602-631, 2011.
[8] D. Pan, B. Kim, L. V. Wang and G. M. Lanza, "A brief account of nanoparticle contrast agents for photoacoustic imaging," *Wiley Interdisciplinary Reviews: Nanomedicine and Nanobiotechnology*, vol. 5, no. 5, pp. 517-543, 2013.
[9] M. Erfanzadeh, P. D. Kumavor and Q. Zhu, "Laser scanning laser diode photoacoustic microscopy system," *Photoacoustics*, vol. 9, pp. 1-9, 2018.
[10] P. K. Upputuri and M. Pramanik, "Pulsed laser diode based optoacoustic imaging of biological tissues," *Biomedical Physics & Engineering Express*, vol. 1, no. 4, pp. 045010, 2015.
[11] P. K. Upputuri and M. Pramanik, "Performance characterization of low-cost, high-speed, portable pulsed laser diode photoacoustic tomography (PLD-PAT) system," *Biomedical optics express*, vol. 6, no. 10, pp. 4118-4129, 2015.
[12] Y. Merkulov and I. Markov, "Ultrasound diagnostic for sturgeon: Practical guideline: 2th edition," *Applied Sturgeon Agency*, ISBN 978-5-6042433-1-2, 2019.
[13] I. C. G. S. Consortium, "Sequence and comparative analysis of the chicken genome provide unique perspectives on vertebrate evolution," *Nature*, vol. 432, pp. 695, 2004.
[14] C. M. Langton and C. F. Njeh, "The physical measurement of bone," *CRC Press*, 2016.
[15] Y. He, B. Gao, A. Sophian, and R. Yang, "Transient electromagnetic-thermal nondestructive testing: pulsed eddy current and transient eddy current thermography," *Butterworth-Heinemann*, 2017.
[16] R. Konrad, N. Padmanaban, K. Molner, E. A. Cooper and G. Wetzstein, "Accommodation-invariant computational near-eye displays," *ACM Transactions on Graphics (TOG)*, vol. 36, no. 4, pp. 88:1-12, 2017.
[17] S. Jäckle, J. Strehlow and S. Heldmann, "Shape Sensing with Fiber Bragg Grating Sensors: A Realistic Model of Curvature Interpolation for Shape Reconstruction," *Bildverarbeitung fur die Medizin*, pp. 258-263, 2019.
[18] T. L. Szabo and P. A. Lewin, "Ultrasound transducer selection in clinical imaging practice," *Journal of Ultrasound in Medicine*, vol. 32, no. 4, pp. 573-582, 2013.
[19] L. Wang and D. R. Suderman, "Application of Batters and Breadings to Various Substrates," in *Batters and Breadings in Food Processing*, ed: Elsevier, pp. 243-261, 2011.
[20] H.-E. Albrecht, N. Damaschke, M. Borys and C. Tropea, "Laser Doppler and phase Doppler measurement techniques," *Springer Science & Business Media*, 2013.
[21] R. B. Thompson and T. Gray, "A model relating ultrasonic scattering measurements through liquid–solid interfaces to unbounded medium scattering amplitudes," *The Journal of the Acoustical Society of America*, vol. 74, pp. 1279-1290, 1983.
[22] Y. Hwu, W.-L. Tsai, A. Groso, G. Margaritondo, and J. H. Je, "Coherence-enhanced synchrotron radiology: simple theory and practical applications," *Journal of Physics D: Applied Physics*, vol. 35, pp. R105, 2002.
[23] P. K. Upputuri and M. Pramanik, "Dynamic in vivo imaging of small animal brain using pulsed laser diode-based photoacoustic tomography system," *Journal of biomedical optics*, vol. 22, no. 9, pp. 1-4., 2017.
[24] J. R. Mayo, W. Webb, R. Gould, M. Stein, I. Bass, G. Gamsu and H. I. Goldberg, "High-resolution CT of the lungs: an optimal approach," *Radiology*, vol. 163, no. 2, pp. 507-510, 1987.
[25] J. N. Stirman, I. T. Smith, M. W. Kudenov and S. L. Smith, "Wide field-of-view, multi-region, two-photon imaging of neuronal activity in the mammalian brain," *Nature biotechnology*, vol. 34, pp. 857-862, 2016.
[26] H. H. Hu, A. J. Madhuranthakam, D. G. Kruger, J. F. Glockner and S. J. Riederer, "Variable field of view for spatial resolution improvement in continuously moving table magnetic resonance imaging," *Magnetic Resonance in Medicine: An Official Journal of the International Society for Magnetic Resonance in Medicine*, vol. 54, no. 1, pp. 146-151, 2005.
[27] M. Koutalonis, H. Delis, A. Pascoal, G. Spyrou, L. Costaridou and G. Panayiotakis, "Can electronic zoom replace magnification in mammography? A comparative Monte Carlo study," *The British journal of radiology*, vol. 83, no. 991, pp. 569-577, 2010.
[28] M. S. Silva, H. P. Alves, J. F. d. Nascimento and J. F. Martins-Filho, "Impact of Pulse Width on the Sensitivity and Range of a Raman-based Distributed Fiberoptic Temperature Sensor," *Journal of Microwaves, Optoelectronics and Electromagnetic Applications*, vol. 17, no. 4, pp. 539-551, 2018.
[29] X. Zeng, S. Yan and G. Wang, "Effects of Microwave Pulse Width on the Spatial Resolution of Microwave-Induced Thermoacoustic Imaging," *2006 7th International Symposium on Antennas, Propagation & EM Theory*, Guilin, pp. 1-4, 2006.
[30] M. Clement, G. Daniel and M. Trelles, "Optimising the design of a broad- band light source for the treatment of skin," *Journal of Cosmetic and Laser Therapy*, vol. 7, no. 3-4, pp. 177-189, 2005.
[31] H. Kawagoe, M. Yamanaka and N. Nishizawa, "Axial resolution and signal-to-noise ratio in deep-tissue imaging with 1.7-μm high-resolution optical coherence tomography with an ultrabroadband laser source," *Journal of biomedical optics*, vol. 22, no. 8, pp. 085002, 2017.
[32] C. J. Thompson and Y. Picard, "Two new strategies to increase the signal to noise ratio in positron volume imaging," in *IEEE Transactions on Nuclear Science*, vol. 40, no. 4, pp. 956-961, 1993.

[33] Liang Zhan et al., "How does angular resolution affect diffusion imaging measures?," *Neuroimage*, vol. 49, no. 2, pp. 1357-1371, 2010.
[34] M. Xu and L. V. Wang, "Analytic explanation of spatial resolution related to bandwidth and detector aperture size in thermoacoustic or photoacoustic reconstruction," *Physical Review E*, vol. 67, no. 5 part 2, pp. 056605, 2003.
[35] A. M. Zysk et al., "Needle-based refractive index measurement using low-coherence interferometry," *Optics letters*, vol. 32, no. 4, pp. 385-387, 2007.

BIOGRAPHIES OF AUTHORS

Hui Ling Chua is currently a research student in Department of Electronic Engineering at Universiti Tun Hussein Onn Malaysia. Her research focuses on photoacoustic imaging for medical diagnostics and tissue characterization. She is a member of Institute of Electrical and Electronics Engineers (IEEE) since 2019.

Audrey Huong is a senior researcher and associate professor at Universiti Tun Hussein Onn Malaysia. Her research interests include noninvasive physiology monitoring of human health, technology development and artificial intelligence assisted clinical diagnosis.